Pattern, style and timing of British–Irish Ice Sheet advance and retreat over the last 45 000 years

Bradwell, Tom; Fabel, Derek; Clark, Chris D.; Chiverrell, Richard C.; Small, David; Smedley, Rachel K.; Saher, Margot H.; Moreton, Steven G.; Dove, Dayton; Callard, S. Louise; Duller, Geoff A.T.; Medialdea, Alicia; Bateman, Mark D.; Burke, Matthew J.; McDonald, Neil; Gilgannon, Sean; Morgan, Sally; Roberts, David H.; Cofaigh, Colm

Published in:
Journal of Quaternary Science

DOI:
10.1002/jqs.3296

Publication date:
2021

Citation for published version (APA):
Bradwell, T., Fabel, D., Clark, C. D., Chiverrell, R. C., Small, D., Smedley, R. K., Saher, M. H., Moreton, S. G., Dove, D., Callard, S. L., Duller, G. A. T., Medialdea, A., Bateman, M. D., Burke, M. J., McDonald, N., Gilgannon, S., Morgan, S., Roberts, D. H., & Cofaigh, C. (2021). Pattern, style and timing of British–Irish Ice Sheet advance and retreat over the last 45 000 years: Evidence from NW Scotland and the adjacent continental shelf. *Journal of Quaternary Science*, *36*(5), 871-933. https://doi.org/10.1002/jqs.3296

Supplementary Information for

Pattern, style and timing of British-Irish Ice Sheet advance and retreat over the last 45,000 years: evidence from NW Scotland and the adjacent continental shelf

Tom Bradwell*, Derek Fabel, Chris D. Clark, Richard C. Chiverrell, David Small, Rachel K. Smedley, Margot Saher, Steven G. Moreton, Dayton Dove, S. Louise Callard, Geoff A.T. Duller, Alicia Medialdea, Mark D. Bateman, Matthew J. Burke, Neil McDonald, Sean Gilgannon, Sally Morgan, David H. Roberts & Colm Ó Cofaigh

*Correspondence to: tom.bradwell@stir.ac.uk

This PDF file includes:

Supplementary Text

1. Notes and Definitions

Absolute ages — we use the term *absolute* here to refer to the fact that all ages in this work are on the same timescale and therefore can be compared in an absolute rather than a relative way. We are aware that all Quaternary age assessments are based on models that may be imperfectly constrained.

ka BP and **ka cal BP** — all ages and dates in the text are expressed in calendar kilo-years before present (ka BP), on a common (or absolute) timescale. In the Results sections, radiocarbon dates are presented in conventional uncalibrated form (in Tables), and subsequently calibrated into calendar kilo-years before present [1950 CE]. For avoidance of doubt, these ages are stated as 'cal ka BP' in the text.

Last glacial cycle — defined here for convenience as Marine Isotope Stages 2-5d (i.e. 116-11.7 ka BP. Broadly equivalent to the Weichselian glacial *Stage* in chronostratigraphic studies of Northern Europe and offshore regions. We do not include the warm Eemian (N European) = Ipswichian (UK) interglacial stage (MIS 5e) in this definition. Note: MIS = Marine Isotope Stage throughout.

Last Glacial Maximum (LGM) — refers to the ***global*** last glacial maximum when eustatic sea levels were at their lowest (100 to 140 m below present) and NH continental ice sheets were generally at their largest (in volume and area). There is no definitive date for this event, however most northern European palaeoglaciological studies now converge on the time period – 23-21 ka BP (e.g. Hughes et al., 2016). Some modellers and sea-level scientists prefer a stricter definition centred ca. 24-26 ka BP (Peltier and Fairbanks, 2007) or ca. 22-19 ka BP (Yokoyama et al., 2018) – when eustatic sea level was at its global minimum. A more relaxed time envelope of ~26-19 ka BP or ~30-19 ka BP is preferred by others, especially when synthesising sea level data with northern and southern hemisphere ice-sheet extent information (e.g. Clark et al., 2009; Carlson & Clark, 2012; Yokoyama et al., 2018). The term *Local Last Glacial Maximum* (LLGM) is sometimes used for specific ice sheets (e.g. Ballantyne & Small, 2018), but this can cause confusion and use of the term 'LLGM' is discouraged.

Greenland Stadials and ice-core chronology — we use the standardised definitions and timings of Greenland Stadials (GS-1, GS-2, etc) and Greenland Interstadials (GI-1, GI-2, etc) throughout this work as recommended by the INTIMATE group (Lowe et al., 2008; Rasmussen et al., 2014). The timescale is defined by the NGRIP isotopic record and uses the Greenland Ice Core Chronology (GICC05), in years before 2000 CE.

Weichselian vs Devensian — we use the term *Weichselian* throughout this work (referring to glacial Stage), covering the time period from 116.0-11.7 ka BP – starting at the onset of GI-25 and ending at the end of GS-1. Weichselian is now the standard Northern European terminology, used throughout Scandinavia, including Iceland, Faroe and adjacent offshore regions. To avoid confusion and ambiguity we do not use the terms *Devensian* glacial Stage or *Dimlington Stadial,* even though these are commonly used by UK-English authors.

2. Bayesian modelling Methods

Two Bayesian temporal models have been developed in this work: one for the mainland-sourced ice sheet and one for Lewis. Both models were developed using OxCal 4.3 (Bronk Ramsey, 2013). The Bayesian analysis uses Markov chain Monte Carlo (MCMC) sampling to build up a distribution of possible solutions generating a probability, called a posterior density estimate for each sample, these are the product of the prior model and likelihood probabilities. This has produced modelled ages for boundaries (Tables 10 & 11) delimiting several zones or phases. Each phase groups dating information for sites that share a common relationship with all other items in the model. Phases are separated by boundary commands, which generate modelled age-probability distributions for Boundary Limits that bracket events within the retreat sequence (Tables 10 & 11).

The sequence model was run in an outlier mode to assess outliers in time using a student's t-distribution ($p < 0.05$) to describe the distribution of outliers with a scaling of 10-10,000 years (Bronk Ramsey, 2009). Complete outliers were given a probability scaling of $p = 1$, with ages showing a poor model fit given values of $p < 0.25$, $p < 0.5$, $p < 0.75$ and $p < 0.90$ on a scale of increasing severity. Outliers here, in part, reflect the site-specific treatments (see Results) but also assess the fit of individual age measurements in the different phases of grouped dating information, as well as their fit in the overall retreat sequence. Chronological measurements showing a strong fit to the model have individual agreement indices >60 (Bronk Ramsey, 2009, 2013) ([A:values] on Fig. 32). Ultimately, Bayesian analysis produced a conformable age model with an overall agreement index of 158% for the Minch Ice Stream and 138% for Lewis, exceeding the 60% threshold advocated by Bronk Ramsey (2009, 2013). Note that ages relating to ice-sheet fluctuations before ~35 ka BP were not included in the Bayesian modelling for reasons of computational complexity.

3. References for Supplementary Information

Ballantyne CK, Small D. 2018. The last Scottish ice sheet. *Earth and Environmental Science Transactions of the Royal Society of Edinburgh* **110**: 93-131.

Bronk Ramsey C. 2013. OxCal 4.3. Manual [online] available at: https://c14.arch.ox.ac.uk/oxcalhelp/hlp_contents.html

Bronk Ramsey C. 2009. Bayesian analysis of radiocarbon dates. *Radiocarbon* **51**: 337-360.

Clark PU, Dyke AS, Shakun JD, Carlson AE, Clark J, Wohlfarth B, Mitrovica JX, Hostetler SW, McCabe AM. 2009. The Last Glacial Maximum. *Science* **325**: 710-714.

Carlson A, Clark PU. 2012. Ice sheet sources of sea level rise and freshwater discharge during the last deglaciation. *Reviews of Geophysics* **50**: RG4007.

Hughes ALC, Gyllencreutz R, Lohne ØS, Mangerud J, Svendsen JI. 2016. The last Eurasian ice sheets – a chronological database and time-slice reconstruction, DATED-1. *Boreas* **45**: 1-45

Lowe JJ, Rasmussen, SO, Bjorck S, Hoek, WZ, Steffensen JP, Walker MJC, Yu ZC. 2008. Synchronisation of palaeo-environmental events in the North Atlantic region during the Last Termination: a revised protocol recommended by the INTIMATE group. *Quaternary Science Reviews* **27**: 6-17.

Rasmussen SO, Bigler M, Blockley SP, Blunier T, Buchardt SL, Clausen HB, Cvijanovic I, Dahl-Jensen D, Johnsen SJ, Fischer H, Gkinis V, Guillevic M, Hoek WZ, Lowe JJ, Pedro JB, Popp T, Seierstad IK, Steffensen JD, Svensson AM, Vallelonga P, Vinther BM, Walker MJC, Wheatley JJ, Winstrup, M. 2014. A stratigraphic framework for abrupt climatic changes during the Last Glacial period based on three synchronized Greenland ice-core records: refining and extending the INTIMATE event stratigraphy. *Quaternary Science Reviews* **106**: 14-28.

Peltier WR, Fairbanks RG. 2007. Global glacial ice volume and Last Glacial Maximum duration from an extended Barbados sea level record. *Quaternary Science Reviews* **25**: 3322-3337.

Yokoyama Y. and 17 others. 2018. Rapid glaciation and a two-step plunge into the Last Glacial Maximum. *Nature* **559**: 603-607.

Supplementary Figures

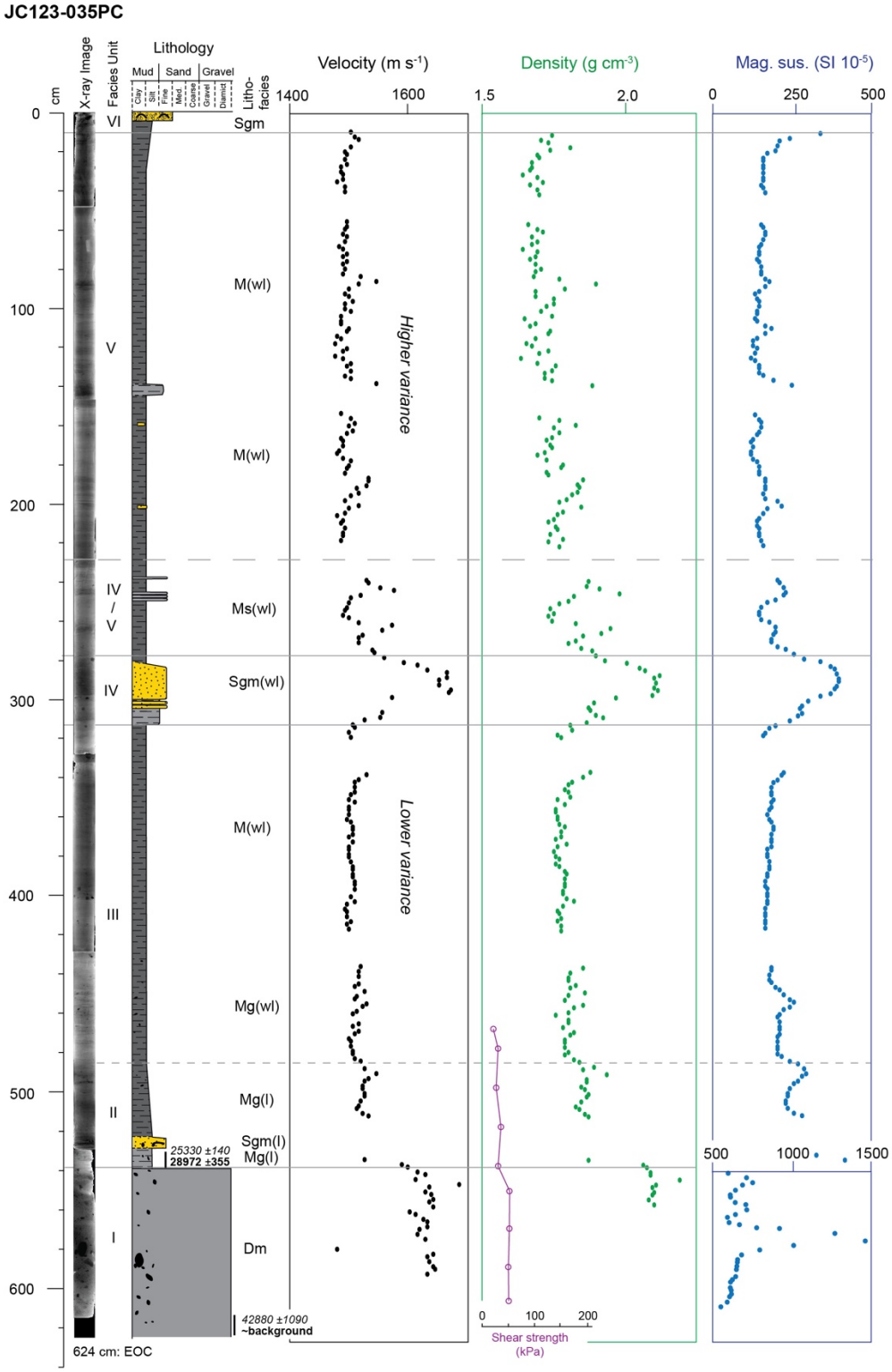

Figure S1: Sedimentology, geochronology and geophysical properties of seabed core **JC123-035VC**. From left to right: X-radiograph, interpreted lithofacies boundaries, lithological log, main lithofacies codes, P-wave velocity, gamma-ray attenuation (density), magnetic susceptibility and undrained shear strength values all plotted on same depth scale. Ages of AMS-dated samples given in radiocarbon years (italic) and calibrated yrs BP (bold font) (see Table 8). Geophysical properties data measured using a Geotek MSCL-S at 2 cm intervals. Gaps are missing data (end caps).

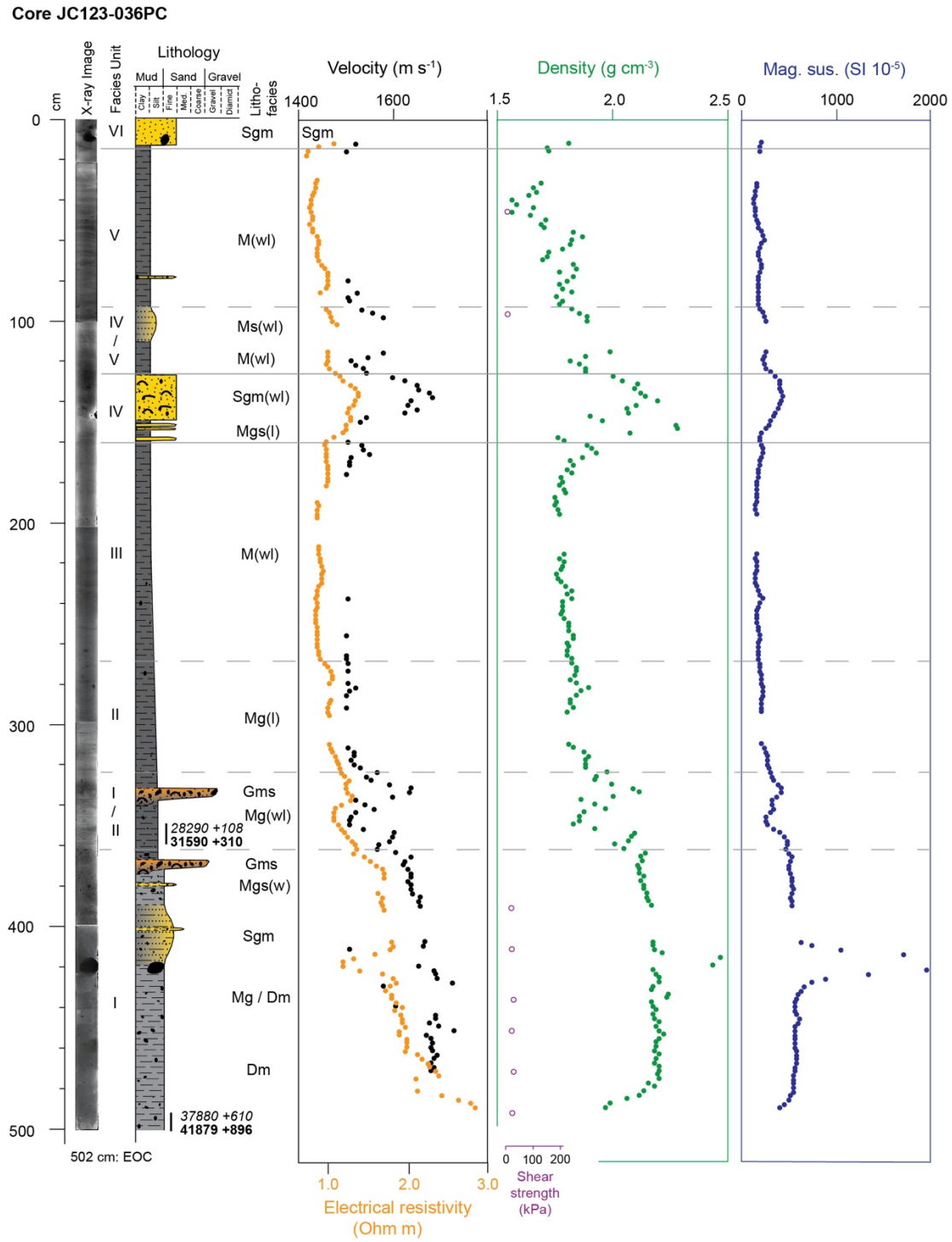

Figure S2: Sedimentology, geochronology and geophysical properties of seabed core **JC123-036VC**. From left to right: X-radiograph, interpreted lithofacies boundaries, lithological log, main lithofacies codes, P-wave velocity, electrical resistivity, gamma-ray attenuation (density) and magnetic susceptibility values all plotted on same depth scale. Ages of AMS-dated samples given in radiocarbon years (italic) and calibrated yrs BP (bold font) (see Table 8). Geophysical properties data measured using a Geotek MSCL-S at 2 cm intervals. Gaps are missing data (end caps).

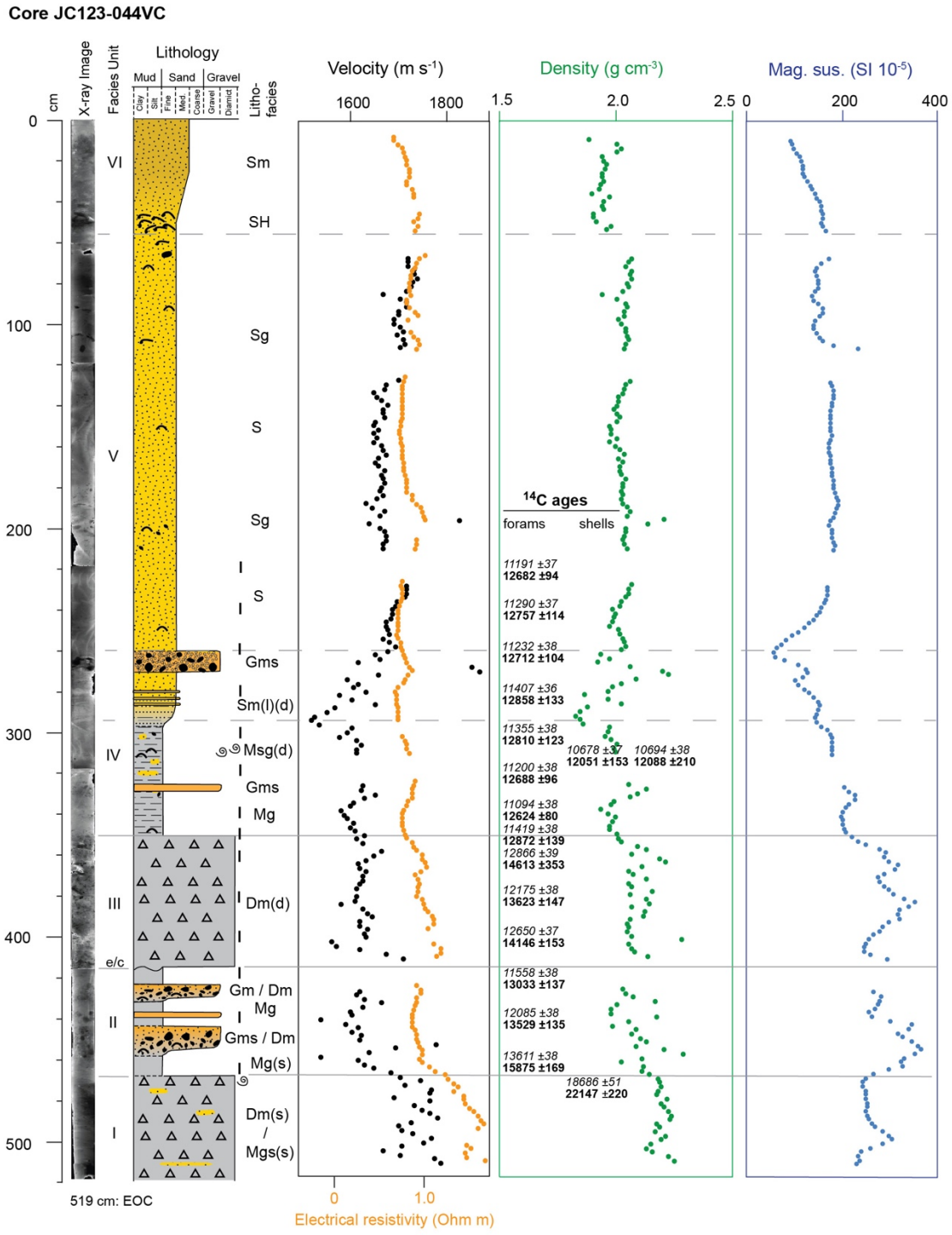

Figure S3: Sedimentology, geochronology and geophysical properties of seabed core **JC123-044VC**. From left to right: positive X-radiograph, interpreted lithofacies boundaries, lithological log, main lithofacies codes, P-wave velocity, electrical resistivity, gamma-ray attenuation (density) and magnetic susceptibility values all plotted on same depth scale. Ages of AMS-dated samples given in radiocarbon years (italic) and calibrated years BP (bold font) with uncertainties (see Table 8). Geophysical properties data measured using a Geotek MSCL-S at 2 cm intervals. Gaps are missing data (end caps). Note: see text for explanation and relevance of chronology

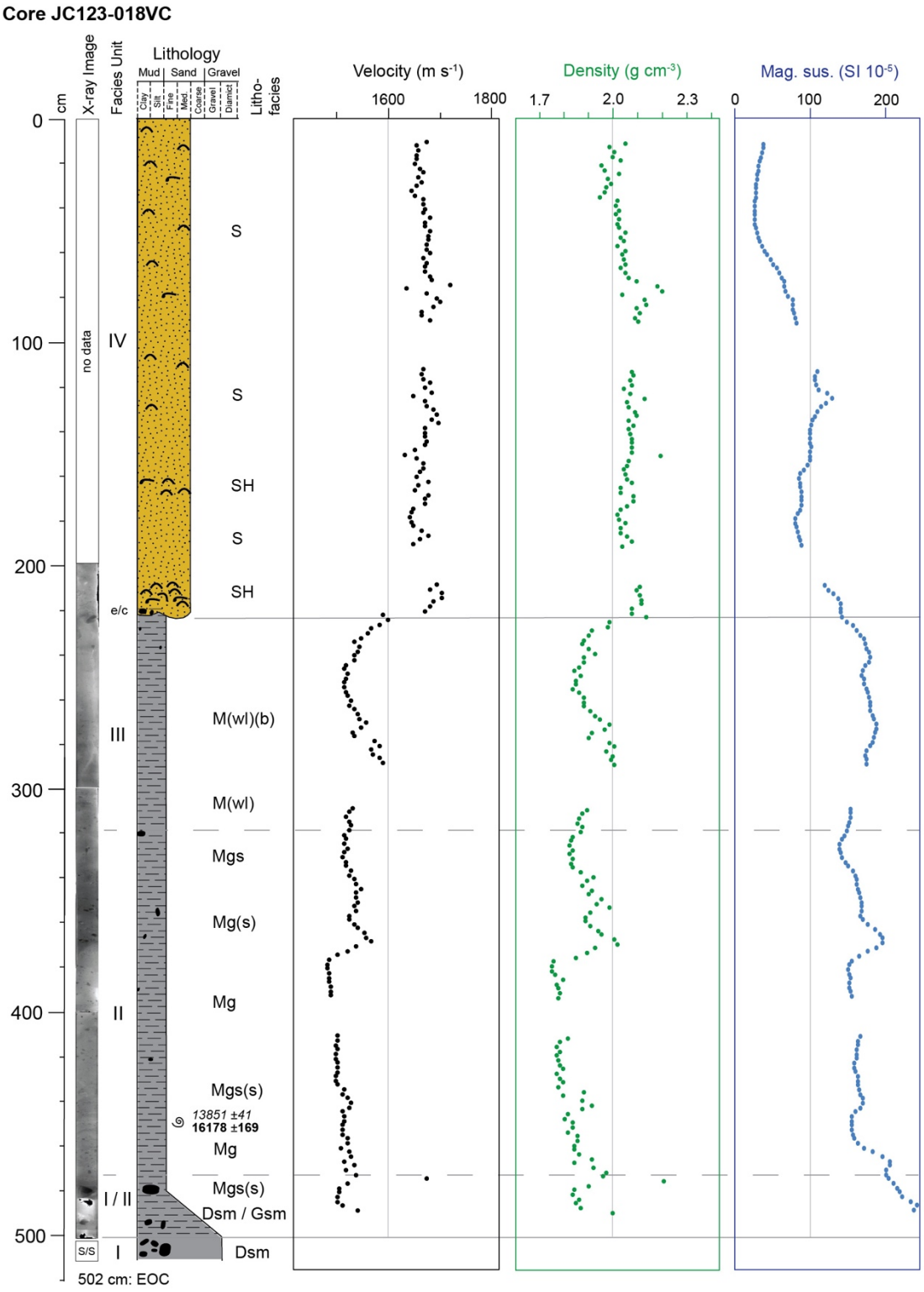

Figure S4: Sedimentology, geochronology and geophysical properties of seabed cores **JC123-018VC**. From left to right: positive X-radiograph, interpreted lithofacies boundaries, lithological log, main lithofacies codes, P-wave velocity, gamma-ray attenuation (density) and magnetic susceptibility values all plotted on same depth scale. Age of AMS-dated sample in radiocarbon years (italic) and calibrated years BP (bold font) with uncertainties (see Table 8). Geophysical properties data measured using a Geotek MSCL-S at 2 cm intervals. Gaps are missing data (end caps).

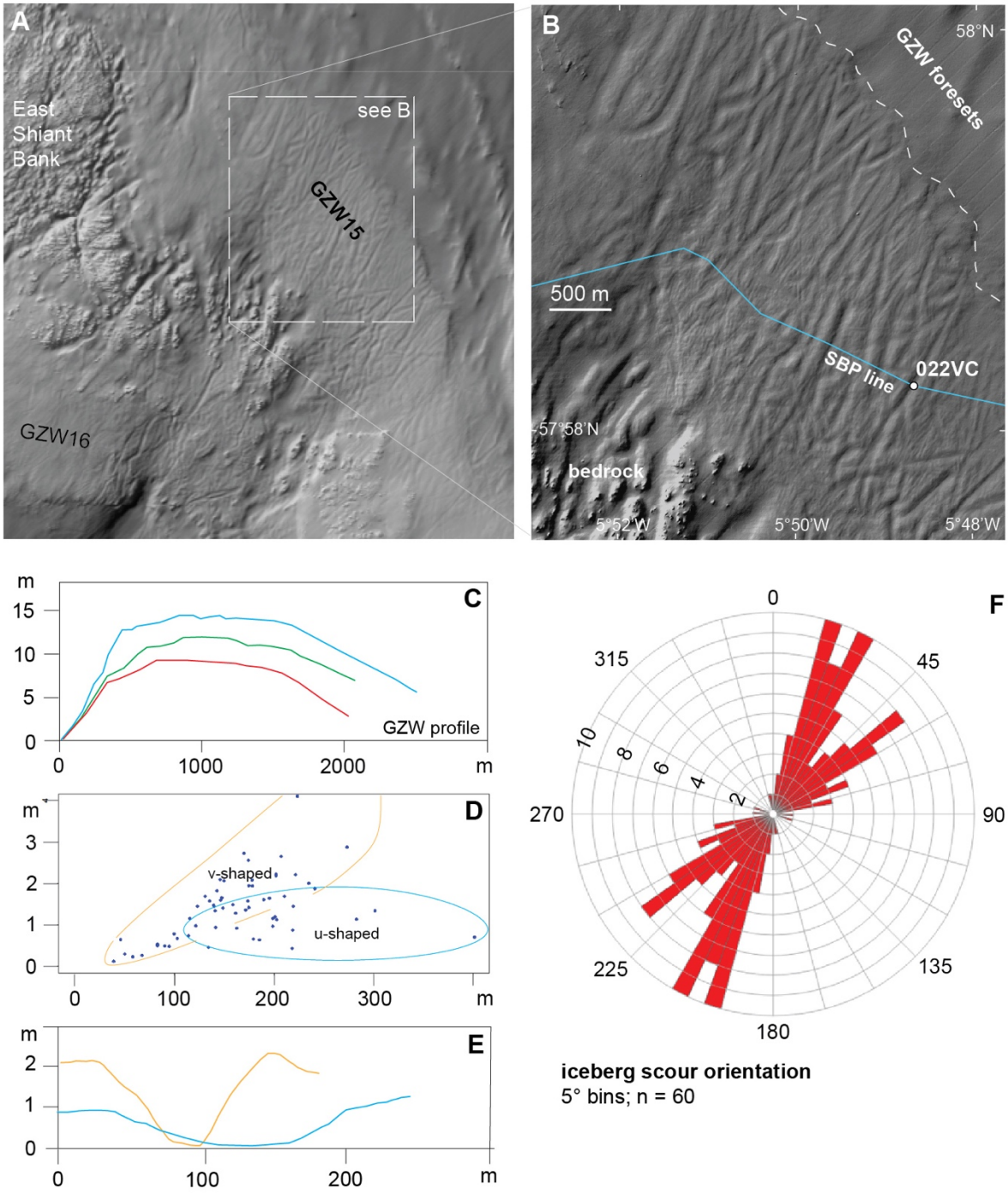

Figure S5: GZW15 – evidence of iceberg scouring and former ice-shelf breakup. A: Hillshaded surface model of MBES data (collected by MCA/UKHO), showing GZW15 and its association with the large submarine bedrock high – the East Shiant Bank. B: Close-up of MBES data, highlighting strongly iceberg-scoured GZW surface. SBP line and core site also shown (see Fig. 27). C: Bathymetric profile across GZW15 (perpendicular to crestline) showing typical geomorphology; red = Q3 profile; green = median; Blue = Q1 profile. D: Scatter plot of ploughmark width vs ploughmark depth (incision into seabed). Note the different width : depth profiles predominantly relating to two different ploughmark types: u- and v-shaped. E: Typical cross profiles of u- and v-shaped iceberg ploughmarks on GZW15. F: Rose diagram showing preferred NNE-NE orientation of iceberg scours on GZW15.

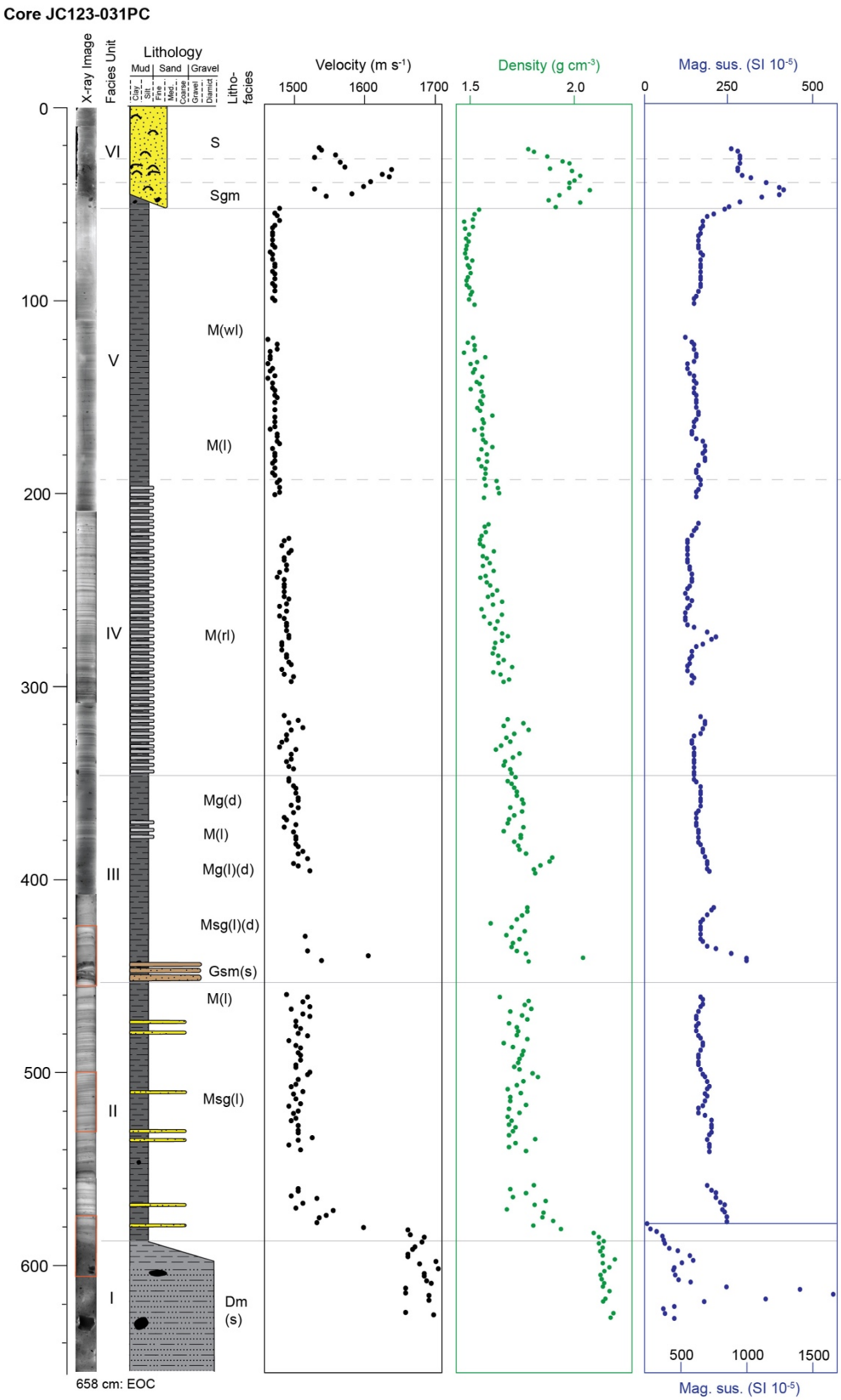

Figure S6: Sedimentology and geophysical properties of seabed core **JC123-031PC**. From left to right: positive X-radiograph, interpreted lithofacies boundaries, lithological log, main lithofacies codes, P-wave velocity, gamma-ray attenuation (density) and magnetic susceptibility values all plotted on same depth scale. Geophysical properties data measured using a Geotek MSCL-S at 2 cm intervals. Gaps are missing data (end caps).

Core JC123-029PC

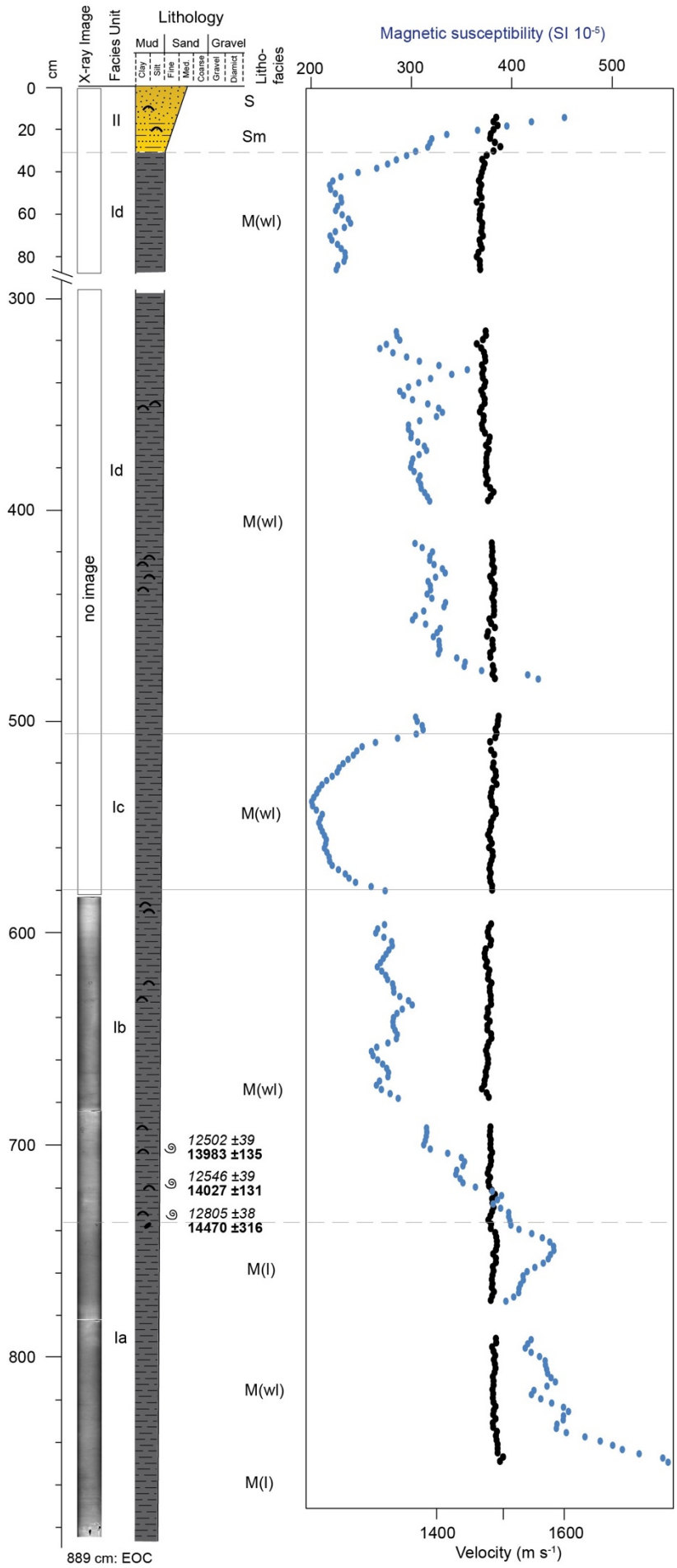

Figure S7: (above) sedimentology, geophysical properties and acoustic stratigraphy of seabed core **JC123-029PC**, Sound of Raasay, Inner Minch. From left to right: positive X-radiograph, interpreted lithofacies boundaries, lithological log, main lithofacies codes, magnetic susceptibility and P-wave velocity values all plotted on same depth scale. Ages of AMS-dated sample in radiocarbon years (italic) and calibrated years BP (bold font) with uncertainties (see Table 8). Geophysical properties data measured using a Geotek MSCL-S at 2 cm intervals. Gaps are missing data (end caps). Note the break between 80-300 cm to allow for Figure to be scaled appropriately on printed page.

Supplementary Data Table S1.

Core metadata						Non-destructive analyses conducted					
Core number	Location [Degrees, decimal minutes]	Location	Water depth (m)	Recovered core length (m)	Curation notes	P-wave velocity	GRA density	Magnetic susceptibility	Electrical resistivity	Photography (split core)	X-radiography (split core)
JC123-002VC	58° 48.264' N 5° 20.845' W	Inner shelf, N of Cape Wrath	89	2.00	2 sections	✓	✓	✓	✓	✓	✓
JC123-003PC	58° 46.800'N 5° 5.866'W	Inner shelf, N of Cape Wrath	101	3.24	4 sections	✓	✓	✓	✓	✓	
JC123-004VC	58° 46.801'N 5° 5.842'W	Inner shelf, N of Cape Wrath	102	4.13	5 sections	✓	✓	✓	✓	✓	✓
JC123-005VC	58° 46.803'N 4° 58.554'W	Inner shelf, N of Cape Wrath	91	1.05	2 sections	✓	✓	✓	✓	✓	
JC123-006VC	58° 45.471'N 6° 16.491'W	Mid-shelf	121	5.06	6 sections	✓	✓	✓	✓	✓	✓
JC123-007VC	58° 42.398'N 6° 10.665'W	Mid-shelf	120	2.82	3 sections	✓	✓	✓	✓	✓	✓
JC123-008VC	58° 42.302'N 6° 10.487'W	Mid-shelf	120	2.82	3 sections	✓	✓	✓	✓	✓	✓
JC123-009VC	58° 42.117'N 6° 10.237'W	Mid-shelf	121	4.38	5 sections	✓	✓	✓	✓	✓	✓
JC123-010VC	58° 40.174'N 6° 6.550'W	Mid-shelf	124	5.37	6 sections	✓	✓	✓	✓	✓	✓
JC123-011VC	58° 35.692'N 5° 58.539'W	Inner Shelf, Outer Minch	112	3.14	4 sections	✓	✓	✓	✓	✓	✓
JC123-012VC	58° 03.916'N 5° 30.818'W	North Minch	70	2.63	3 sections	✓	✓	✓	✓	✓	✓
JC123-013VC	58° 05.627'N 5° 30.520'W	North Minch	67	3.77	4 sections	✓	✓	✓	✓	✓	
JC123-014VC	58° 05.932'N 5° 31.428'W	North Minch	52	1.73	2 sections	✓	✓	✓	✓	✓	
JC123-015VC	58° 09.731'N 5° 30.080'W	North Minch	119	3.9	4 sections	✓	✓	✓	✓	✓	✓
JC123-016VC	58° 10.927'N 5° 31.550'W	North Minch	102	5.59	6 sections	✓	✓	✓	✓	✓	
JC123-017VC	58° 23.162'N 5° 28.879'W	North Minch	118	5.07	6 sections	✓	✓	✓	✓	✓	
JC123-018VC	58° 22.261'N 5° 27.272'W	North Minch	113	5	5 sections	✓	✓	✓	✓	✓	✓
JC123-019VC	58° 21.826'N 5° 25.417'W	North Minch	111	1.38	2 sections	✓	✓	✓	✓	✓	
JC123-020PC	57° 57.936'N 5° 45.553'W	Inner Minch	116	6.93	8 sections	✓	✓	✓	✓	✓	✓

JC123-021PC	57° 58.179'N 5° 47.135'W	Inner Minch	105	8.69	9 sections	✓	✓	✓	✓	✓	✓
JC123-022VC	57° 58.275'N 5° 48.621'W	Inner Minch	83	4.67	5 sections	✓	✓	✓	✓	✓	✓
JC123-023VC (see note)	57° 58.885'N 5° 50.478'W	Inner Minch	95	0	No recovery						
JC123-029PC	57° 33.455'N 6° 5.809'W	Inner Minch	84	8.89	10 sections	✓	✓	✓	✓	✓	✓
JC123-030VC	57° 33.458'N 6° 5.825'W	Inner Minch	84	0	No recovery						
JC123-031PC	57° 55.128'N 6° 13.793'W	Inner Minch	120	6.635	7 sections	✓	✓	✓	✓	✓	✓
JC123-032PC	57° 55.512'N 6° 13.949'W	Inner Minch	118	7.215	8 sections	✓	✓	✓	✓	✓	✓
JC123-033PC	57° 58.448'N 6° 15.310'W	Inner Minch	101	8.22	9 sections	✓	✓	✓	✓	✓	✓
JC123-034PC	58° 04.536'N 6° 14.237'W	North Minch	100	6.445	7 sections	✓	✓	✓	✓	✓	✓
JC123-035PC	59° 11.731'N 7° 14.932'W	Continental Slope	525	6.33	7 sections	✓	✓	✓	✓	✓	✓
JC123-036PC	59° 11.156'N 7° 14.698'W	Continental Slope	491	5.01	6 sections	✓	✓	✓	✓	✓	✓
JC123-037VC	59° 10.958'N 7° 14.603'W	Continental Slope	484	4.15	5 sections	✓	✓	✓	✓	✓	✓
JC123-038VC	59° 10.686'N 7° 14.391'W	Continental Slope	457	4.8	5 sections	✓	✓	✓	✓	✓	✓
JC123-039VC	59° 05.633'N 7° 8.433'W	Outer Shelf	183	4	4 sections	✓	✓	✓	✓	✓	✓
JC123-040VC	59° 07.530'N 6° 50.612'W	Outer Shelf	175	6.06	6 sections	✓	✓	✓	✓	✓	✓
JC123-041VC	59° 07.470'N 6° 50.747'W	Outer Shelf	175	1.01	2 sections	✓	✓	✓	✓	✓	
JC123-042PC	58° 56.230'N 6° 53.270'W	Outer Shelf	171	0.47	1 section	✓	✓	✓	✓	✓	
JC123-043VC	58° 56.232'N 6° 53.274'W	Outer Shelf	171	4.59	5 sections	✓	✓	✓	✓	✓	✓
JC123-044VC	58° 55.605'N 6° 52.141'W	Outer Shelf	164	5.2	6 sections	✓	✓	✓	✓	✓	✓
JC123-045VC	58° 51.425'N 6° 37.983'W	Inner Shelf	143	4.93	5 sections	✓	✓	✓	✓	✓	✓
JC123-046VC	58° 44.167'N 6° 12.319'W	Mid-Shelf	112	0.86	1 section	✓	✓	✓	✓	✓	
JC123-047VC	58° 46.804'N 4° 50.719'W	Inner shelf, N of Cape Wrath	88	0	No recovery						

JC123-048VC	58° 46.805'N 4° 50.715'W	Inner shelf, N of Cape Wrath	89	3.66	4 sections	✓	✓	✓	✓	✓	✓
JC123-049VC	58° 46.801'N 4° 48.325'W	Inner shelf, N of Cape Wrath	86	2.48	3 sections	✓	✓	✓	✓	✓	✓
JC123-050VC	58° 46.798'N 4° 42.289'W	Inner shelf, N of Cape Wrath	82	1.52	2 sections	✓	✓	✓	✓	✓	
JC123-051VC	58° 46.806'N 4° 40.458'W	Inner shelf, N of Cape Wrath	84	1.94	2 sections	✓	✓	✓	✓	✓	

Note: Vibrocorer deployments JC123-023VC to JC123-028VC failed to recover any sediment owing to a vibrocorer malfunction.

Boundary Limit (event bracketed)	**Median modelled age (ka) with uncertainties (2σ)**
Base of sequence	38.6 ± 4.4
BL0 (start of MnIS advance)	31.4 ± 2.6
BL1 (Shelf-edge maximum)	29.7 ± 1.9
BL2 (Retreat to GZW2)	27.7 ± 1.0
BL3 (Retreat to GZW3; N. Lewis moraine)	25.2 ± 2.1
BL4 (Retreat to Cape Wrath)	22.9 ± 1.3
BL5 (Retreat to Tolsta, NE Lewis)	21.4 ± 1.7
BL6 (Retreat to Eye Peninsula)	19.0 ± 1.6
BL7 (W MnIS collapse end; retreat to E Lewis/Harris Coast)	17.3 ± 0.9
BL8 (East Minch Readvance end)	15.4 ± 1.5
BL9 (Retreat to N Raasay)	14.3 ± 2.2
BL10 (Retreat to central Raasay)	15.6 ± 0.8
BL11 (Retreat to Strollamus; WRR advance)	14.9 ± 1.0
BL12 (Retreat from WRR)	13.9 ± 1.6
BL13 (Retreat to Loch Broom)	14.6 ± 0.6
End of sequence	12.8 ± 2.2

Table S2: Bayesian age-modelled boundaries: Minch Ice Stream (main BIIS).

Boundary Limit (event bracketed)	**Median modelled age (ka) with uncertainties (2σ)**
Base of sequence	31.4 ± 2.6
BL1 (retreat to Skigersta, N Lewis)	22.7 ± 0.9
BL2 (retreat to Ard Bheag Bragar)	20.1 ± 0.9
BL3 (retreat to Bragar / Islibhig)	18.0 ± 0.7
BL4 (retreat to Uig Hills, W Lewis)	16.1 ± 1.0
End of sequence	13.8 ± 1.1

Table S3: Bayesian age-modelled boundaries: Lewis (Outer Hebrides)-centered ice mass.